ANALYTICAL SCIENCES JULY 2015, VOL. 31

Multi-walled Carbon Nanotubes/Graphite Nanosheets Modified Glassy Carbon Electrode for the Simultaneous Determination of Acetaminophen and Dopamine

Susu ZHANG, Ping HE,† Guangli ZHANG, Wen LEI, and Huichao HE

School of Materials Science and Engineering, Southwest University of Science and Technology, State Key Laboratory Cultivation Base for Nonmetal Composites and Functional Materials, Mianyang 621010, Sichuan, P. R. China

Graphite nanosheets prepared by thermal expansion and successive sonication were utilized for the construction of a multi-walled carbon nanotubes/graphite nanosheets based amperometric sensing platform to simultaneously determine acetaminophen and dopamine in the presence of ascorbic acid in physiological conditions. The synergistic effect of multi-walled carbon nanotubes and graphite nanosheets catalyzed the electrooxidation of acetaminophen and dopamine, leading to a remarkable potential difference up to 200 mV. The as-prepared modified electrode exhibited linear responses to acetaminophen and dopamine in the concentration ranges of 2.0×10^{-6} – 2.4×10^{-4} M ($R = 0.999$) and 2.0×10^{-6} – 2.0×10^{-4} M ($R = 0.998$), respectively. The detection limits were down to 2.3×10^{-7} M for acetaminophen and 3.5×10^{-7} M for dopamine ($S/N = 3$). Based on the simple preparation and prominent electrochemical properties, the obtained multi-walled carbon nanotubes/graphite nanosheets modified electrode would be a good candidate for the determination of acetaminophen and dopamine without the interference of ascorbic acid.

Keywords Acetaminophen, dopamine, graphite nanosheets, multi-walled carbon nanotubes, electroanalysis

(Received October 11, 2014; Accepted January 26, 2015; Published July 10, 2015)

Introduction

Acetaminophen (AC) is a long-established analgesic and antipyretic drug used to relieve pain and reduce fever, especially for patients who are susceptible to aspirin.[1] At normal therapeutic doses, AC is completely metabolized to inactive metabolites that are eliminated in the urine. However, overdosage of AC leads to accumulation of toxic metabolites and causes acute hepatotoxicity and nephrotoxicity.[2] Hence, it is essential to establish an appropriate method to determine medicament levels of AC with high selectivity and sensitivity.

In view of the clinical significances of AC and the coexisting relationship to some neurotransmitters in biological fluids, especially dopamine (DA), attempts have been made to determine AC and DA both individually and simultaneously by various techniques, including spectroscopy, chromatography, capillary electrophoresis and flow-injection analysis.[3-6] Generally speaking, the above techniques are complicated, time-consuming and/or usually require specialized instruments. The electroanalytical method is comparatively simple and efficient for the determination of AC or DA due to its high sensitivity, satisfactory stability and low cost.[7,8] However, if AC and DA are coexisting in one system, their oxidation peak potentials overlap significantly on many electrodes. In order to improve the selectivity, it is essential to separate the signals from each other. Nowadays, chemically and physically-modified electrodes are used to meet these demands. They include multi-walled carbon nanotubes modified glassy carbon electrode (MWCNTs/GCE),[9] nano-TiO_2/polymer coated GCE,[10] Ruthenium Red-MWCNTs modified GCE[11] and gold nanoparticles modified carbon paste electrode.[12]

Carbon materials are widely used in electroanalysis due to their considerable electrocatalytic activity.[13] Possessing high specific surface area and excellent electrical conductivity, MWCNTs have been widely employed for the construction of electrochemical sensors to improve analytical responses.[14] However, in addition to the limitations of high cost and the ease of forming aggregates, the lack of defect sites of MWCNTs will result in poor electrochemical performance.[15] To address this, several strategies for dispersing MWCNTs have been developed.[16-18] At the same time, efforts have been made to combine other materials with MWCNTs, aiming to make compensations for the lack of defect sites.[19,20] As one kind of carbon nanomaterial, graphite nanosheets (GNSs) can be prepared by exfoliating graphite powders at low cost and, moreover, they show excellent electrochemical performance because of the large number of edge defect sites.[21] GNSs present large numbers of edge defect sites and high disorder degree, which is conductive to exhibit excellent electrocalalytic activity similar to graphene. Although some reports about the application of GNSs in supercapacitors and lithium ion batteries are available, few papers report their application in electrochemical sensors. However, there exists the irreversible agglomeration resulting from inadequate intercalation during

† To whom correspondence should be addressed.
E-mail: heping@swust.edu.cn

preparation.[22] Upon dispersing MWCNTs with GNSs, the conductivity can be improved and the restacking of GNSs can be prevented.[23] Furthermore, large numbers of edge defect sites of GNSs are adequately present and help to realize the excellent electrochemical performance.

Herein, based on the combination of advantages of MWCNTs and GNSs, we prepared MWCNTs/GNSs modified GCE for the simultaneous determination of AC and DA in the presence of ascorbic acid (AA). The as-prepared amperometric sensor presented satisfactory sensitivity and selectivity, excellent reproducibility and long-time stability because of the synergistic effect of MWCNTs and GNSs. The detection limits were down to 2.3×10^{-7} M for AC and 3.5×10^{-7} M for DA ($S/N = 3$), respectively, in the presence of AA.

Experimental

Chemicals and reagents

MWCNTs (>98% purity) and graphite powders were purchased from Chengdu Organic Chemicals Co., Ltd., Chinese Academy of Sciences (Chengdu, China). A supply of 5 wt% Nafion solution was purchased from Aldrich Chemical Reagent Co., Ltd..

The obtained AC, DA, AA, Na_2HPO_4 and KH_2PO_4 were analytical grade and purchased from Chengdu Chemical Reagent Co., Ltd. (Chengdu, China). Stock solutions of 5.0×10^{-3} M DA, AC and AA were kept in an ice bath. Phosphate buffer solution (PBS, pH 6.8) was prepared by mixing stock solutions of Na_2HPO_4 and KH_2PO_4 (0.10 M, volume ratio = 1:1). Supporting electrolytes were prepared by using doubly distilled deionized water and before each experiment the solutions were deoxygenated by purging with pre-purified nitrogen gas for 10 min.

Pretreatment of MWCNTs and preparation of GNSs

First, 5.0 g MWCNTs were refluxed at 80°C for 3 h in a flask containing concentrated sulfuric acid and nitric acid with volume ratio of 3:1. The acid-treated MWCNTs were washed repeatedly with doubly distilled water until the filtrate became neutral and then dried at 80°C overnight.

GNSs were prepared as follows.[24] Graphite powders were placed into a mixture of concentrated sulfuric acid and nitric acid with volume ratio of 4:1 and stirred for 24 h at room temperature. The acid-treated graphite powders were washed with doubly distilled water until the filtrate became neutral and dried at 80°C overnight. The acid-treated intercalated graphite powders were heat-treated at 900°C for 30 s to expand layer-to-layer spacing and then cooled down to room temperature naturally. The expanded graphite was immersed in 70% alcohol solution and sonicated successively for 8 h. Finally, the dispersed GNSs were filtered and dried until the solvent volatilized completely.

Materials characterization

Fourier transform infrared (FTIR) spectra of raw MWCNTs and treated MWCNTs were recorded with an FTIR spectrometer (Nicolet-5700, USA) in wavenumber range of 1000 – 4000 cm^{-1} using KBr sheets. The crystal structure of graphite powders and GNSs were characterized by a Raman spectrometer (INVIA, England) in wavenumber range of 1000 – 2000 cm^{-1}. The morphology of GNSs was obtained using a scanning electron microscope (Ultra 55, Zesis Corp.).

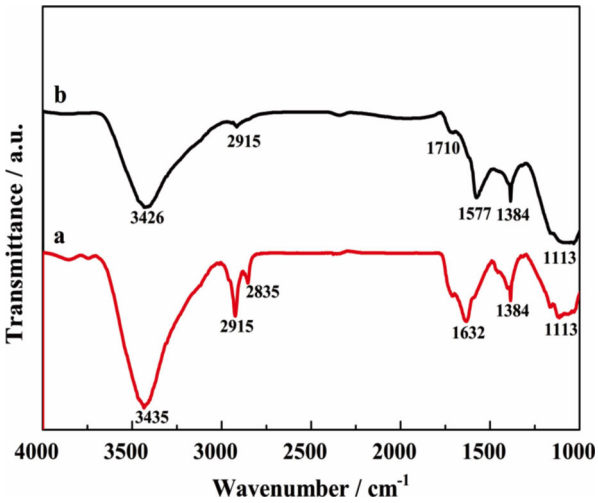

Fig. 1 FTIR spectra of raw MWCNTs (a) and treated MWCNTs (b).

Electrode preparation and electrochemical characterization

Prior to electrode modification, the GCE was polished to a mirror finish with 0.50 and 0.050 μm alumina powders successively and then washed by sonication in doubly distilled water repeatedly.

Next, 2.5 mg MWCNTs and 2.5 mg GNSs were dispersed into 1.0 mL 1% Nafion solution to form a homogenous mixture by sonication. MWCNTs/GNSs/GCE was prepared by casting 5.0 μL MWCNTs/GNSs suspension on GCE and then was dried in air. The procedures to prepare MWCNTs/GCE and GNSs/GCE were similar to that of MWCNTs/GNSs/GCE, just replacing MWCNTs/GNSs suspension with MWCNTs and GNSs suspension.

Cyclic voltammogram (CV) and differential pulse voltammogram (DPV) were recorded with a CHI 760C electrochemical workstation by introducing a three-electrode test system using a platinum electrode as the counter electrode, bare or modified GCE as the working electrode referred to saturated calomel electrode (SCE). For DPV experiment, the parameters were as follows: increment potential of each point = 0.004 V, potential pulse amplitude = 0.05 V, potential pulse width = 0.05 s, data sampling width = 0.0167 s and potential pulse period = 0.2 s.

Results and Discussion

FTIR spectral characterization

Shown in Fig. 1 are FTIR spectra of raw MWCNTs (a) and treated MWCNTs (b). As observed in Fig. 1a, the peak at 3435 cm^{-1} was attributed to the presence of –OH group, which could appear either from ambient moisture bound to MWCNTs or during the purification of raw materials.[25] The peaks at 2915 and 2835 cm^{-1} were assigned to the stretching vibration of the C–H bond of the alkyl group.[26] The peaks at 1632 and 1384 cm^{-1} were due to the stretching vibrations of C=C and C–C bonds, respectively. The peak at 1113 cm^{-1} represented the stretching vibration of the C–O bond.[27] Compared with the FTIR spectrum of raw MWCNTs, peaks at 3426, 1710 and 1577 cm^{-1} in Fig. 1b were assigned to –OH stretching vibration of –COOH, C=O stretching vibration of –COOH and C=C stretching vibration near –COOH group, respectively, indicating that large numbers of –COOH groups at the end and sidewall of nanotubes were

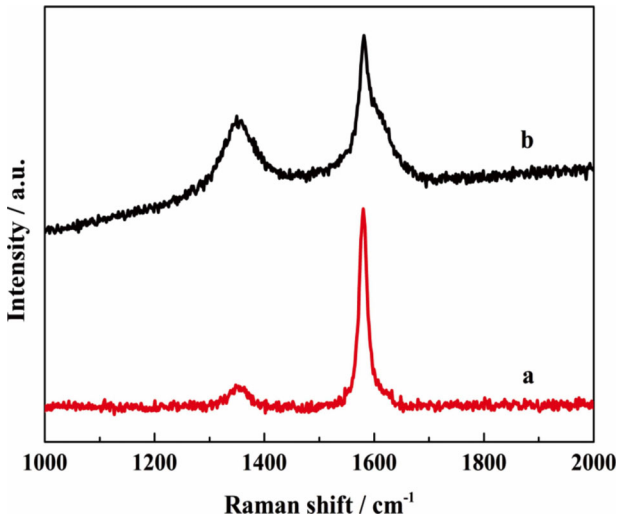

Fig. 2 Raman spectra of graphite powders (a) and GNSs (b).

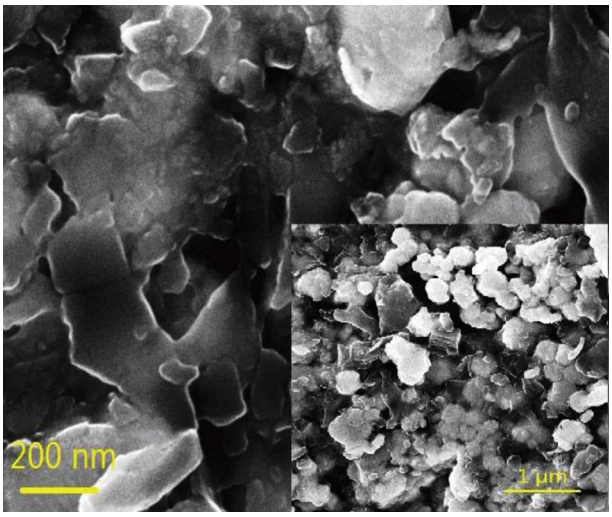

Fig. 3 SEM image of GNSs. Inset shows the SEM image of GNSs with low magnification.

present after concentrated acid oxidation treatment.[28]

Raman spectral characterization

Raman spectrum is a nondestructive tool usually utilized to characterize carbonaceous materials. As shown in Fig. 2, Raman spectra of both graphite powders and GNSs showed D-band at 1350 cm^{-1} due to the breathing mode of *k*-point phonons of A_{1g} symmetry and G-band at 1580 cm^{-1} corresponding to the first-order scattering of E_{2g}, respectively.[29] The intensity ratio of D and G bands, I_D/I_G, usually indicated a disorder degree and was proportional to the degree of structural defects.[30] It was observed that, by oxidation treatment of graphite powders, the G-band of as-prepared GNSs was broadened and the relative intensity of the D-band was increased due to the presence of the crystalline-sheet structure. I_D/I_G value was calculated as 0.17 for raw graphite powders, while I_D/I_G value increased to 0.70 for GNSs, indicating the presence of larger numbers of edge defect sites and higher disorder degree.[31]

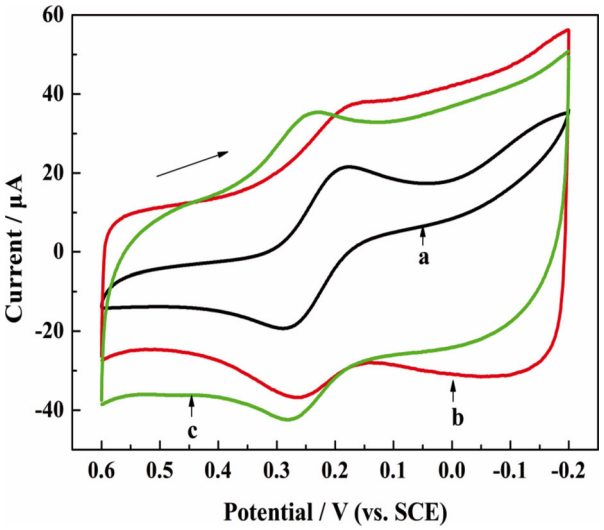

Fig. 4 CVs of 1.0 mM $K_3Fe(CN)_6$ + 0.10 M KCl solution on GNSs/GCE (a), MWCNTs/GCE (b) and MWCNTs/GNSs/GCE (c). Scan rate: 50 mV s^{-1}.

Morphological characterization

Shown in Fig. 3 is the SEM image of as-prepared GNSs. It was revealed that the expanded graphite was completely torn to sheets with a thickness of 30 – 80 nm and two-dimensional size of 100 – 900 nm, and the edges of GNSs were clearly observed. The edge defect sites and high disorder of GNSs were in accordance with Raman characterization, which were responsible for the excellent electrochemical performance.

CV characterization of modified electrodes

Usually, $[Fe(CN)_6]^{3-/4-}$ is used as a electrochemical probe to test the electron transfer kinetic between electrode and the species in solution. Potential difference of anodic and cathodic peaks (ΔE_p) is usually used to evaluate electron transfer kinetics.[32] Shown in Fig. 4 are CVs of 1.0 mM $K_3Fe(CN)_6$ in 0.10 M KCl solution on bare GCE and as-prepared modified electrodes. It was found that ΔE_p of 112 mV on GNSs/GCE (Fig. 4a) was larger than that obtained on bare GCE (65 mV, not shown herein), suggesting that $[Fe(CN)_6]^{3-/4-}$ redox couple had a slow electron transfer kinetics on GNSs, possibly due to the presence of negatively charged oxygen-containing moieties on the surface of GNSs and the poor conductivity of GNSs.[33,34] In addition, ΔE_p of the $[Fe(CN)_6]^{3-/4-}$ probe on MWCNTs/GCE (Fig. 4b) decreased to 93 mV, which was related to the fine electrical conductivity of MWCNTs and was beneficial to facilitate electron transfer between $[Fe(CN)_6]^{3-/4-}$ ions and electrode.[35] More remarkably as shown in Fig. 4c, the smallest ΔE_p of 58 mV was obtained for the $[Fe(CN)_6]^{3-/4-}$ probe on MWCNTs/GNSs/GCE, which was because that MWCNTs acted as effective electron conduction pathway and prevented GNSs from restacking. Meanwhile, large numbers of edges of GNSs assisted fast electron transfer between $[Fe(CN)_6]^{3-/4-}$ ions and the electrode.[36]

Electrochemical behavior of AC and DA

Shown in Fig. 5 are CVs of AC and DA on bare GCE and as-prepared modified electrodes in 0.10 M PBS buffer solution. It was well known that the electrochemical determination of AC in the presence of DA on bare GCE was difficult because of the overlapped voltammetric responses.[37] In Fig. 5a, there appears

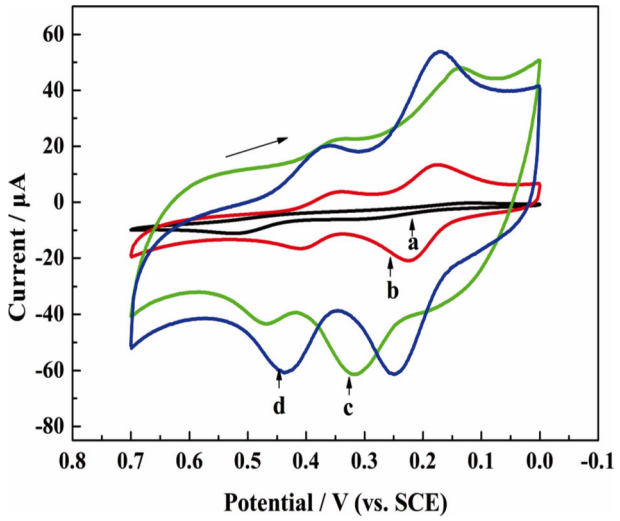

Fig. 5 CVs of 2.0×10^{-4} M AC and 2.0×10^{-4} M DA on GCE (a), GNSs/GCE (b), MWCNTs/GCE (c) and MWCNTs/GNSs/GCE (d) in 0.10 M PBS buffer (pH 6.8). Scan rate: 50 mV s^{-1}.

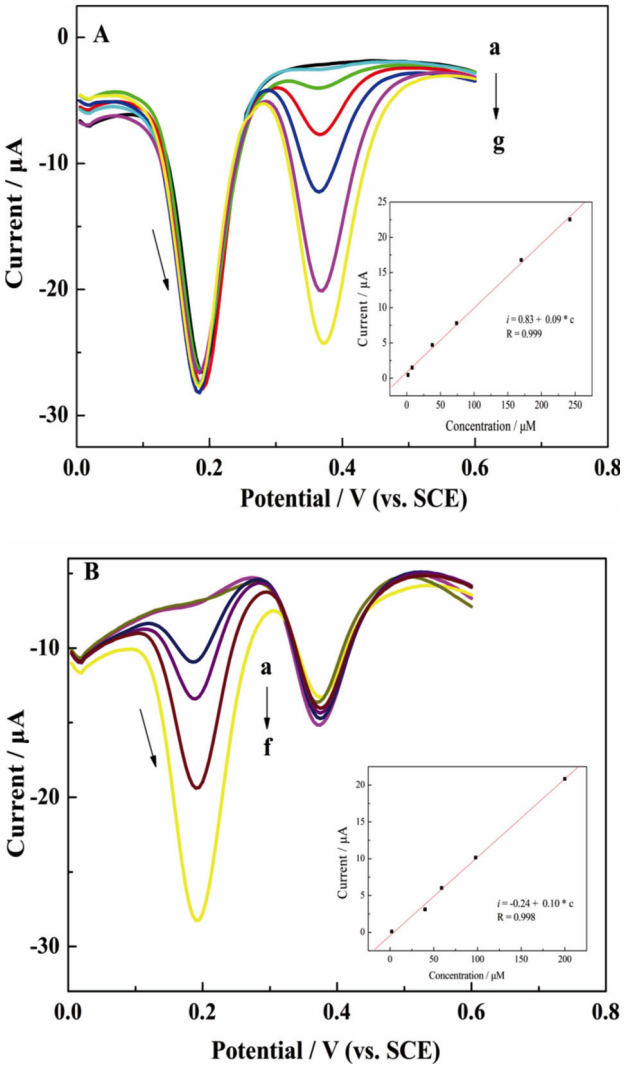

Fig. 6 DPVs of AC and DA on MWCNTs/GNSs/GCE in 0.10 M PBS buffer (pH 6.8). (A) 2.0×10^{-4} M DA and varying concentrations of AC (a-g): 0, 2.0×10^{-6}, 8.0×10^{-6}, 3.8×10^{-5}, 7.4×10^{-5}, 1.7×10^{-4} and 2.4×10^{-4} M. (B) 1.0×10^{-4} M AC and varying concentrations of DA (a – f): 0, 2.0×10^{-6}, 4.0×10^{-5}, 5.9×10^{-5}, 9.8×10^{-5} and 2.0×10^{-4} M. Insets show the linear calibration plots of currents *versus* concentrations.

were two couples of broad and overlapped peaks on bare GCE, while the peak potentials of AC and DA were nearly indistinguishable. When GCE was modified with GNSs, the overlapped voltammetric peaks of AC and DA were resolved into two couples of well-defined peaks (Fig. 5b) and, moreover, the oxidation peak potentials of both AC and DA were negatively shifted compared to those on bare GCE, suggesting that the edge defect sites promoted electrocatalysis towards the oxidation of AC and DA simultaneously.[21] Observed in the CV curve on MWCNTs/GCE (Fig. 5c) was a higher current than that on bare GCE, indicating that the presence of MWCNTs could effectively improve conductivity and was beneficial to improve sensitivity.[38] As for the CV curve on MWCNTs/GNSs/GCE (Fig. 5d), remarkably higher amperometric responses and lower overpotentials were observed. The excellent electrocatalytic effect might be attributed to the following reasons. On one hand, MWCNTs could show efficient electrocatalysis towards AC and DA owning to its good conductivity. On the other hand, GNSs provided abundant edge defect sites, making great contributions to the electrocatalytic effect. Hence, the synergistic effect of MWCNTs and GNSs might offer a favorable microenvironment for electroactive species through the formation of a 3D conductive network, which was beneficial for accelerating electron transfer between the modified electrode and species in solution.[39]

The effect of scan rates on peak currents of AC and DA on MWCNTs/GNSs/GCE was investigated in pH 6.8 PBS buffer (not shown here). Both oxidation and reduction currents of AC at about 445 and 375 mV were linear with square root of potential scan rates. Similarly, for DA, linear relationships of both oxidation and reduction currents at about 245 and 175 mV *versus* square root of potential scan rates were also obtained. Therefore, it was demonstrated that electrochemical processes of both AC and DA were diffusion-controlled.

Simultaneous determination of AC and DA

Shown in Fig. 6 are DPVs of AC and DA on MWCNTs/GNSs/GCE in 0.10 M PBS buffer (pH 6.8). Obviously, two well-separated oxidation peaks were observed at 0.40 V for AC and 0.20 V for DA. Figure 6A shows that peak currents of AC increased with AC concentrations while the concentration of DA was kept constant at 2.0×10^{-4} M. The linear regression equation for AC was $i_{pa}/\mu A = 0.83 + 0.09 \times c/\mu M$ in the range of 2.0×10^{-6} – 2.4×10^{-4} M ($R = 0.999$). Similarly, voltammetric determination of DA was carried out in the presence of AC at a fixed concentration of 1.0×10^{-4} M (Fig. 6B). The oxidation peak currents of DA were linear with concentrations in the range of 2.0×10^{-6} – 2.0×10^{-4} M, and the linear equation could be calculated as $i_{pa}/\mu A = -0.24 + 0.10 \times c/\mu M$ ($R = 0.998$). The detection limits were calculated as 2.3×10^{-7} M for AC and 3.5×10^{-7} M for DA ($S/N = 3$), respectively. It was indicated that the as-prepared MWCNTs/GNSs/GCE in this work had high sensitivity and selectivity for the simultaneous determination of AC and DA.

Interference

One of the main difficulties in the development of a modified

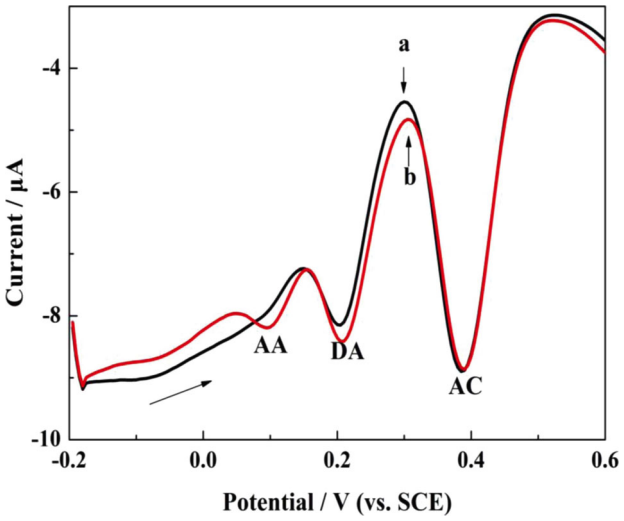

Fig. 7 DPVs of 1.0×10^{-5} M DA and 5.0×10^{-5} M AC on MWCNTs/GNSs/GCE in the absence of AA (a) and presence of 1.0×10^{-4} M AA (b) in 0.10 M PBS buffer (pH 6.8).

electrode for the determination of AC and/or DA was interference due to AA.[40,41] Shown in Fig. 7 are DPVs of 1.0×10^{-5} M DA and 5.0×10^{-5} M AC on MWCNTs/GNSs/GCE in the absence of AA and presence of 1.0×10^{-4} M AA in 0.10 M PBS buffer (pH 6.8). It was found that well-distinguished peaks for AA, DA and AC were obtained with large potential difference and, furthermore, oxidation currents of DA and AC remained nearly constant even in the presence of AA with high concentration, indicating that it could be possible to selectively detect AC and DA in the presence of AA on MWCNTs/GNSs/GCE. It should be noted that the oxidation current of AA at a potential of 0.10 V increased with the concentration. However, the linear response between oxidation current and concentration of AA was somewhat unsatisfactory, so the electroanalysis application of AA in the presence of DA and AC was not discussed in this work.

Stability and reproducibility

Stability and reproducibility were important properties to characterize the performance of the modified electrode. Thus, stability and reproducibility of analytical signals for DA and AC in the presence of AA on MWCNTs/GNSs/GCE was studied over two weeks. It was found that the as-prepared MWCNTs/GNSs/GCE gave RSDs of 4.3 and 4.9% ($n = 10$) for the determination of 2.0×10^{-4} M AC and 2.0×10^{-4} M DA, respectively. The results above showed that the as-prepared MWCNTs/GNSs/GCE had long-time stability and good reproducibility for the determination of AC and DA.

Conclusions

The voltammetric results reported in this paper clearly demonstrated that the simultaneous determination of AC and DA without the interference of AA was successfully achieved on MWCNTs/GNSs/GCE. The synergistic effect of MWCNTs and GNSs catalyzed the electrooxidation of AC and DA, leading to a remarkable potential difference. The detection limits were down to 2.3×10^{-7} M for AC and 3.5×10^{-7} M for DA ($S/N = 3$). The as-prepared modified electrode showed desirable characteristics including low cost, good stability and reproducibility and satisfactory sensitivity, and it could be a good candidate for the determination of AC and DA with quite promising results.

Acknowledgements

We are grateful to anonymous reviewers for their helpful and insightful comments. This work was supported by the Open Project of the State Key Laboratory Cultivation Base for Nonmetal Composites and Functional Materials, School of Materials Science and Engineering, Southwest University of Science and Technology, Sichuan Province, China (11zxfk26); and the Technology R&D Program of Sichuan Province (No. 2010GZ0300). Also we are grateful for the help of the Analytical and Testing Center of Southwest University of Science and Technology, Sichuan Province, China.

References

1. M. S. M. Quintino, K. Araki, H. E. Toma, and L. Angnes, *Electroanalysis*, **2002**, *14*, 1629.
2. M. E. Bosch, A. J. R. Sanchez, F. S. Rojas, and C. B. Ojeda, *J. Pharm. Biomed. Anal.*, **2006**, *42*, 291.
3. M. R. Moghadam, S. Dadfarnia, A. M. H. Shabani, and P. Shahbazikhah, *Anal. Biochem.*, **2011**, *410*, 289.
4. E. McEvoy, S. Donegan, J. Power, and K. Altria, *J. Pharm. Biomed. Anal.*, **2007**, *44*, 137.
5. S. E. Gibbons, C. Wang, and Y. F. Ma, *Talanta*, **2011**, *84*, 1163.
6. P. Fanjul-Bolado, P. J. Lamas-Ardisana, D. Hernandez-Santos, and A. Costa-Garcia, *Anal. Chim. Acta*, **2009**, *638*, 133.
7. N. F. Atta, M. F. El-Kady, and A. Galal, *Sens. Actuators, B*, **2009**, *141*, 566.
8. J. J. Gooding, *Electroanalysis*, **2008**, *20*, 573.
9. A. Kutluay and M. Aslanoglu, *Sens. Actuators, B*, **2013**, *185*, 398.
10. S. A. Kumar, C. F. Tang, and S. M. Chen, *Talanta*, **2008**, *76*, 997.
11. H. H. Nadiki, M. Noroozifar, and M. Khorasani-Motlagh, *Anal. Sci.*, **2014**, *30*, 911.
12. N. F. Atta, A. Galal, F. M. Abu-Attia, and S. M. Azab, *J. Mater. Chem.*, **2011**, *21*, 13015.
13. D. Kato and O. Niwa, *Anal. Sci.*, **2013**, *79*, 385.
14. Y. Liu, Y. Liu, H. B. Feng, Y. M. Wu, L. Joshi, X. Q. Zeng, and J. H. Li, *Biosens. Bioelectron.*, **2012**, *35*, 63.
15. C. L. Fu, W. S. Yang, X. Chen, and D. G. Evans, *Electrochem. Commun.*, **2009**, *11*, 997.
16. K. J. Chen, K. C. Pillai, J. Rick, C. J. Pan, S. H. Wang, C. C. Liu, and B. J. Hwang, *Biosens. Bioelectron.*, **2012**, *33*, 120.
17. Z. H. Wen, S. Q. Ci, and J. H. Li, *J. Phys. Chem. C*, **2009**, *113*, 13482.
18. P. R. Dalmasso, M. L. Pedano, and G. A. Rivas, *Sens. Actuators, B*, **2012**, *173*, 732.
19. J. Yang, W. D. Zhang, and S. Gunasekaran, *Biosens. Bioelectron.*, **2010**, *26*, 279.
20. Y. Y. Yu, Z. G. Chen, S. J. He, B. B. Zhang, X. C. Li, and M. C. Yao, *Biosens. Bioelectron.*, **2014**, *52*, 147.
21. S. M. Chen, W. S. Yang, and X. Chen, *Electroanalysis*, **2010**, *22*, 908.
22. G. H. Chen, C. L. Wu, W. G. Weng, D. J. Wu, and W. L.

Yan, *Polymer*, **2003**, *44*, 1781.
23. R. I. Jafri, T. Arockiados, N. Rajalakshmi, and S. Ramaprabhu, *J. Electrochem. Soc.*, **2010**, *157*, 874.
24. G. H. Chen, D. J. Wu, W. G. Weng, and C. L. Wu, *Carbon*, **2003**, *41*, 579.
25. T. Ramanathan, F. T. Fisher, R. S. Ruoff, and L. C. Brinson, *Chem. Mater.*, **2005**, *17*, 1290.
26. A. N. Chakoli, J. Wan, J. T. Feng, M. Amirian, J. H. Sui, and W. Cai, *Appl. Surf. Sci.*, **2009**, *256*, 170.
27. E. Murugan and G. Vimala, *J. Colloid Interface Sci.*, **2011**, *357*, 354.
28. J. Chen, M. A. Hamon, H. Hu, Y. S. Chen, A. M. Rao, P. C. Eklund, and R. C. Haddon, *Science*, **1998**, *282*, 95.
29. A. C. Ferrari and J. Robertson, *Phys. Rev. B*, **2000**, *61*, 14095.
30. V. Chandra, J. Park, Y. Chun, J. W. Lee, I. C. Hwang, and K. S. Kim, *ACS Nano*, **2010**, *4*, 3979.
31. X. Li and G. H. Chen, *Mater. Lett.*, **2009**, *63*, 930.
32. S. S. Zhang, P. He, W. Lei, and G. L. Zhang, *J. Electroanal. Chem.*, **2014**, *724*, 29.
33. D. Li, M. B. Mueller, S. Gilje, R. B. Kaner, and G. G. Wallace, *Nat. Nanotechnol.*, **2008**, *3*, 101.
34. J. F. Wang, S. L. Yang, D. Y. Guo, P. Yu, D. Li, J. S. Ye, and L. Q. Mao, *Electrochem. Commun.*, **2009**, *11*, 1892.
35. H. G. Nie, Z. Yao, X. M. Zhou, Z. Yang, and S. M. Huang, *Biosens. Bioelectron.*, **2011**, *30*, 28.
36. C. Y. Li, Z. Li, H. W. Zhu, K. L. Wang, J. Q. Wei, X. Li, P. Z. Sun, H. Zhang, and D. H. Wu, *J. Phys. Chem. C*, **2010**, *114*, 14008.
37. B. Habibi, M. Jahanbakhshi, and M. H. Pournaghi-Azar, *Electrochim. Acta*, **2011**, *56*, 2888.
38. A. C. Pereira, M. R. Aguiar, A. Kisner, D. V. Macedo, and L. T. Kubota, *Sens. Actuators, B*, **2007**, *124*, 269.
39. M. Arvand and T. M. Gholizadeh, *Colloids Surf. B*, **2013**, *103*, 84.
40. K. Inada, K. Nishiyama, and I. Taniguchi, *Chem. Lett.*, **2009**, *38*, 814.
41. Y. X. Li, Q. F. Lu, A. B. Shi, Y. L. Chen, S. N. Wu, and L. Wang, *Anal. Sci*., **2011**, *27*, 921.